1-1-2011

Interpolation of the GNSS Wet Troposphere Delay

Johnny Lo
Edith Cowan University

Ahmed El-Mowafy
Curtin University

Proceedings of the SURVEYING & SPATIAL SCIENCES BIENNIAL CONFERENCE 2011
21-25 November 2011, Wellington, New Zealand

Interpolation of the GNSS Wet Troposphere Delay

Johnny Lo
School of Engineering, Edith Cowan University
Perth, WA, Australia
J.Lo@ecu.edu.au

Ahmed El-Mowafy
Department of Spatial Sciences, Curtin University
Perth, WA, Australia
A.El-mowafy@curtin.edu.au

ABSTRACT

Troposphere delay is one of the main distance-dependent errors in Global Navigation Satellite Systems (GNSS) observations. Precise estimation of the troposphere wet delay is necessary to aid ambiguity resolution and for positioning in network Real-Time Kinematic (RTK) and Precise Point Positioning. Wet tropospheric estimates can also serve as a source of atmospheric information to facilitate weather forecasting. Interpolation of the troposphere wet delay is thus required when its estimation is interrupted for short periods or when data are processed at higher intervals from that of available data. The objective of this research is to compare the performance of several interpolation methods that can be used in order to suggest the most appropriate technique. Six interpolation models were considered. The models ranged from the easy-to-implement linear model, to the more sophisticated Kriging model. Other models considered are the cubic spline interpolation, cubic Hermite polynomial interpolation, Lagrange polynomial interpolation, and Fast Fourier transform interpolation. The performance of these methods was assessed by comparing their results with actual troposphere wet delay data collected at the station Onsala (ONSA) in Sweden. As the number of observations used to generate the interpolation process affects the determination of the model coefficients; the use of different lengths of observations was investigated. The number of missing wet delay values considered for interpolation during testing ranged from one to four in a row.

Test results showed that the linear interpolation, the cubic Hermite polynomial and fast Fourier transform models produce better estimates than splines and ordinary Kriging. The Lagrange polynomials method was the poorest performer. The paper provides explanation of the interpolation results achieved by linking them with autocorrelation of the troposphere wet delays.

KEYWORDS: 1. GNSS 2. Precise Positioning 2. Troposphere wet Delay 4. Interpolation

1 INTRODUCTION

Signal delays induced by the troposphere are generally known as tropospheric refractions or tropospheric delays. A tropospheric delay can be divided into hydrostatic (dry) and wet components. In GNSS data processing at a specific site, instead of dealing with multiple tropospheric delays along line-of-sights between the receiver and each satellite, these delays are usually mapped to a single value along the zenith direction using a mapping function. The zenith hydrostatic delay (ZHD) can be estimated with external models to within a millimetre in accuracy (e.g., Saastamoinen, 1972), and be subtracted from the estimated tropospheric delay, leaving behind the zenith wet delay (ZWD) component, which is mostly due to the atmospheric water vapour. The ZWD can then be used to determine the precipitable water vapour (PWV) for a given

site. A receiver at a nearby location can also make use of this ZWD estimates for accurate positioning.

Although the wet delay accounts for only 10% of the total delay, it is far more difficult to model or remove due to the lack of knowledge regarding the distribution of the water vapour in the atmosphere. The temporal and spatial variability of the water vapour ensures that the wet delay cannot be consistently modelled with millimetre precision by any existing tropospheric model. The Global Navigation Satellite System (GNSS) and water vapour radiometers (WVRs) are two of the most effective tools in estimating atmospheric ZWD. Both techniques are able to estimate the ZWD to within 10 mm or less than 2 mm in PWV (e.g., Haefele et al., 2004; Liu et al., 2005; Mattioli et al., 2005; Wang et al., 2007). Once estimated, the ZWD can be applied in other GNSS-related areas such as near real-time or real-time kinematic (RTK) GNSS applications. If a network of reference stations (or a single reference station) is able to provide accurate and precise ZWD estimates in a timely manner, these estimates can then be used by a mobile or static user at an unknown location to improve ambiguity resolution, and ultimately, the position solutions.

The benefits of good tropospheric solutions can also extend to aiding Numerical Weather Prediction (NWP) models to provide better weather forecasts. The impact of GNSS PWV estimates on weather forecasting is well documented (e.g., Kuo et al., 1996; Vedel and Huang, 2003; Gutman et al., 2004; Vedel and Huang, 2004; Smith et al., 2006; Macpherson et al., 2007). These studies reported improvements in the humidity and precipitation forecasts when GNSS PWV estimates are assimilated into NWP models. Comparisons between the estimates from a NWP model with and without GNSS PWV estimates assimilation were made and the improvement in relative humidity (RH) forecasts lead to a 40% reduction of forecast errors (Gutman and Benjamin, 2001). The impact of GNSS PWV estimates was further emphasised by a multi-year experiment over the period from 1999-2004 by Smith et al. (2006), whereby improvements were evident in the 6-h and 12-h RH forecasts.

A well-defined statistical description for the GNSS-derived tropospheric estimates is important for NWP modelling. The autocorrelations describe the temporal correlations between pairs of GNSS tropospheric estimates in a time series (TS), as a function of time differences (Borre and Tiberius, 2000). These correlations need to be defined for the eventual assimilation of the GNSS tropospheric estimates into NWP model, especially for the weighting of past data in a bias reduction scheme (e.g., Stoew et al., 2007). Furthermore, the autocorrelation time length can be used in recursive data processing procedures such as GM Kalman filtering (KF) with state vector augmentation (e.g., Borre and Tiberius, 2000). Studying the autocorrelation of ZWD can also help in selection of the proper model for its interpolation at a specific instance between known values in the time domain.

2 AUTOCORRELATION OF ZENITH WET DELAY

To better understand the temporal correlations that exist among the tropospheric delay estimates, autocorrelation analysis of the ZWD values estimated from WVR is performed over station ONSA in Sweden, which is also an International GNSS Service (IGS) station. The WVR at ONSA was appropriate for this study as it provided ZWD data at a high frequency (every 8 seconds). In this autocorrelation study, WVR ZWD were sampled every hour and at every 10-min interval. These data were analysed with a 12-h time interval and over three different days on September 10th, 13th and 16th in 2003. A 12-h window ensures a first-order stationarity in the Time Series (TS) of data. Stationary TS refers to a process whose parameters, such as the mean and variance, remain fairly constant over time and space (Wei, 2006). Hence, the corresponding autocorrelation of a stationary TS value can then be deemed constant in any time interval within the 12-h window. The autocorrelation plots are given by Figures 1-3. In these figures, autocorrelation values that lie between the red dotted lines, which represent a 95% confidence interval, are deemed insignificant. Each unit of lag for the left-sided figures represents a 1 hour period and for the right-sided figures the unit lag is a 10-min period. The summary statistics for both the 1-h ZWD and 10-min ZWD data sets are given in Table 1. The results of the autocorrelation analysis between the ZWDs, sampled at different rates, were then compared and summarised in Table 2.

Table 1 Mean and standard deviation (cm) of the WVR ZWD sampled at different time intervals

Sampling Rate	Mean and Standard Deviation (cm)		
	Sep-10	Sep-13	Sep-16
10-min	13.5 (1.3)	10.4 (1.0)	13.0 (2.8)
1-h	13.6 (1.5)	10.4 (1.0)	13.1 (3.1)

Table 2 Comparison between the time lengths for significant autocorrelation of the WVR ZWD sampled at different time intervals

Sampling Rate	Time length with Significant Autocorrelation		
	Sep-10	Sep-13	Sep-16
10-min	1-h 30-min	1-h 50-min	2-h
1-h	1-h	1-h	2-h

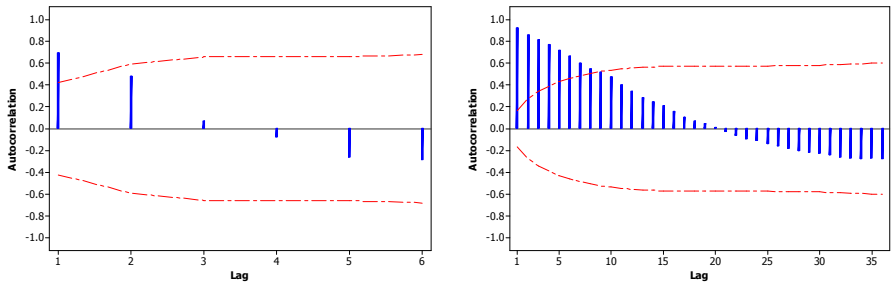

Figure 1: Autocorrelation plot of WVR ZWDs, sampled hourly (left) and at every 10-min interval (right), over ONSA on Sept 10

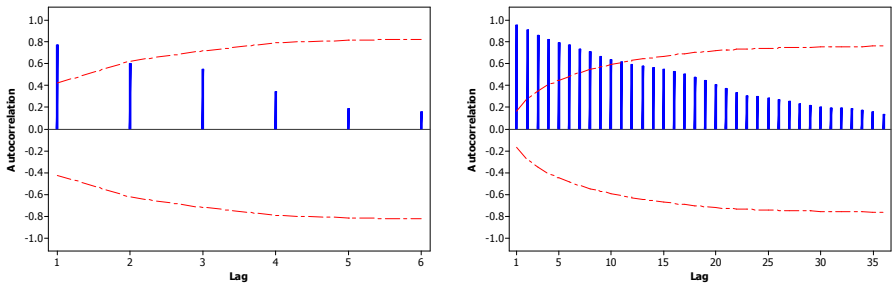

Figure 2: Autocorrelation plot of WVR ZWDs, sampled hourly (left) and at every 10-min interval (right), over ONSA on Sept 13

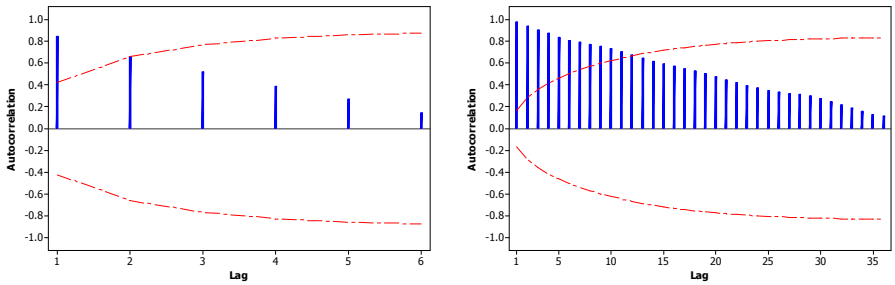

Figure 3: Autocorrelation plot of WVR ZWDs, sampled hourly (left) and at every 10-min interval (right), over ONSA on Sept 16

Although the analysis of 10-min WVR ZWDs involved a greater number of observations than the hourly ZWDs (72 total observations as compared to 12), there are minimal differences between the means and standard deviations of the two sets of data (Table 1). Comparison between Figures 1-3 also shows that the shape of the autocorrelation plots are maintained even when greater number of observations is sampled within the same period. Similarities between the time lengths for significant correlation are also observed for both sets of data in Table 2. On Sept 10th and 13th, both data sets agreed that the autocorrelations are insignificant when the lag is greater than 2-h. However, the 10-min ZWD data set appeared to provide a more precise estimate of the autocorrelation time lag due to the higher sampling rate.

The results above show that the existence of autocorrelations among the tropospheric estimates is evident. The autocorrelations are generally significant for estimates that are within the 1-h to 2-h lag. An average lag value of 1.7 hours is observed at ONSA. Based on these autocorrelation results, the following sections will investigate several possible interpolation methods for ZWD estimates.

3 INTERPOLATION OF ZENITH WET DELAYS

Six models are considered in this study for interpolation of ZWDs. The descriptions of these models are outlined briefly in the following sub-sections. The models range from the easy-to-implement linear interpolant, to an ordinary linear Kriging model. For the purpose of this investigation, the actual and estimated ZWD at time t_i (where i = 0, 1, …, n) are denoted as $ZWD(t_i)$ and $\hat{ZWD}(t_i)$, respectively, where (n+1) is the total number of ZWD values. A set of (n+1) ZWD observations is denoted by $\{ZWD(t_i)\}_{i=0}^{n}$; t_k denotes the time at which it is required to interpolate a value for ZWD.

3.1 Linear Interpolation

The linear interpolation (LI) method fits a linear function between each pair of ZWD points $\{ZWD(t_i), ZWD(t_{i+1})\}$ and returns the values of the estimated ZWD, $\hat{ZWD}(t_k)$, at a specified value of time t_k, where $t_i < t_k < t_{i+1}$ (e.g., Benesty et al., 2004). The estimated ZWD can be formulated as:

$$\hat{ZWD}(t_k) = m(t_k - t_i) + ZWD(t_i) \tag{1}$$

where

$$m = \frac{ZWD(t_{i+1}) - ZWD(t_i)}{t_{i+1} - t_i} \tag{2}$$

3.2 Cubic Spline Interpolation

For a set of $\{ZWD(t_i)\}_{i=0}^{n}$ observations, a cubic spline (CS) ZWD interpolant, $\hat{ZWD}(t_k)$, between the time interval $[t_i, t_{i+1}]$ can be given as (e.g., Burden and Faires, 2004):

$$\hat{ZWD}(t_k) = a_i + b_i(t_k - t_i) + c_i(t_k - t_i)^2 + d_i(t_k - t_i)^3, \text{ for } i = 0, 1, ..., n-1 \tag{3}$$

where,

$$a_i = ZWD(t_i);\ b_i = \frac{(a_{i+1} - a_i)}{h_i} - \frac{h_i(2c_i + c_{i+1})}{3};\ d_i = \frac{(c_{i+1} - c_i)}{3h_i};\ h_i = t_{i+1} - t_i \tag{4}$$

The coefficients $\{c_i\}_{i=0}^{n-1}$ are determined by solving a linear system of equations given by:

$$h_{i-1}c_{i-1} + 2(h_{i-1}h_i)c_i + h_i c_{i+1} = \frac{3(a_{i+1} - a_i)}{h_i} - \frac{3(a_i - a_{i-1})}{h_{i-1}}, \text{ for } i = 0, 1, ..., n-1 \quad (5)$$

To implement the CS interpolation a minimum of three ZWD observations are needed.

3.3 Cubic Hermite Polynomial Interpolation

For any pair of epochs $[t_i, t_{i+1}]$, the cubic Hermite polynomial (CHP) interpolant, $\hat{ZWD}(t_k)$, between the given points can be estimated as (e.g., Burden and Faires, 2004):

$$\hat{ZWD}(t_k) = ZWD(t_i) + f_1(t_k - t_i) + f_2(t_k - t_i)^2 + f_3(t_k - t_i)^2(t_k - t_{i+1}) \quad (6)$$

where,

$$f_1 = \frac{ZWD(t_i) - ZWD(t_{i-1})}{t_i - t_{i-1}};\ f_2 = \frac{f_4 - f_1}{t_{i+1} - t_i};\ f_3 = \frac{f_6 - f_2}{t_{i+1} - t_i};$$
$$f_4 = \frac{ZWD(t_{i+1}) - ZWD(t_i)}{t_{i+1} - t_i};\ f_5 = \frac{ZWD(t_{i+2}) - ZWD(t_{+1i})}{t_{i+2} - t_{i+1}};\ f_6 = \frac{f_5 - f_4}{t_{i+1} - t_i} \quad (7)$$

3.4 Lagrange Polynomial Interpolation

For a set of $\{ZWD(t_i)\}_{i=0}^{n}$ observations there exists a unique polynomial $P(t)$ of a degree $\leq n$ such that (Burden and Faires, 2004):

$$\hat{ZWD}(t_k) = P(t_k) \text{ for each } i = 0, 1, \ldots, n-1 \quad (8)$$

The Lagrange polynomial (LP) is given by:

$$P(t_k) = ZWD(t_0)L_{n,0}(t_k) + \cdots + ZWD(t_n)L_{n,n}(t_k) = \sum_{i=0}^{n} ZWD(t_i)L_{n,i}(t_k) \quad (9)$$

where

$$L_{n,i}(t_k) = \frac{(t_k - t_0)(t_k - t_1)\cdots(t_k - t_{i-1})(t_k - t_{i+1})\cdots(t_k - t_n)}{(t_i - t_0)(t_i - t_1)\cdots(t_i - t_{i-1})(t_i - t_{i+1})\cdots(t_i - t_n)} = \prod_{\substack{j=0 \\ j \neq i}}^{n} \frac{(t_k - t_j)}{(t_i - t_j)} \quad (10)$$

3.5 Fast Fourier Transform Interpolation

To use the fast Fourier transform (FFT) method for the interpolation of the ZWDs, a vector of ZWD observations $[ZWD] = \{ZWD(t_i)\}_{i=1}^{n}$ of length n (sampled at equally spaced points) is firstly transformed to the discrete Fourier transform vector F_{ZWD} using the algorithm given by (Frigo and Johnson, 1998):

$$F_{ZWD} = \sum_{i=1}^{n} ZWD(t_i)v_n^{(i-1)(t-1)} \quad (11)$$

where v_n is the complex n^{th} root of unity (with $j = \sqrt{-1}$) defined by:

$$v_n = e^{-2\pi j/n} \quad (12)$$

The next step of the process is to calculate the inverse Fourier transform vector $\left[Z\hat{W}D\right]=\left\{Z\hat{W}D(t_i)\right\}_{i=1}^{N}$, i.e. the interpolated value) by using the following expression for a user-specified value of N:

$$\left[Z\hat{W}D\right]=\left(\frac{1}{N}\right)\sum_{i=1}^{N}F_{ZWD}\,v_N^{-(i-1)(t-1)} \tag{13}$$

If $n<N$, the vector F_{ZWD} is padded with trailing zeros to a length of N, prior to applying the inverse transformation defined by Eq. (13). If $n>N$, F_{ZWD} is truncated to the specified length. In this investigation, N is given as:

$$N=n\times(\text{number of interpolated observations}) \tag{14}$$

3.6 Ordinary One-dimension Kriging Interpolation

Kriging's method is known as a best linear unbiased estimator as it estimates the value of a random function at a point as a linear combination of the values at the sample points whilst minimizing the error variance. The method assumes that the closer the input parameters are, the more correlated the observations are. With this concept, it is then worthwhile exploring whether Kriging is appropriate as ZWD interpolator whereby time *t* is the input parameter. More precisely, the use of *ordinary* Kriging is investigated in its simplest one-dimensional form to determine its usefulness for interpolating ZWD.

Ordinary Kriging interpolation is performed by using a two-component predictor. The first component can be viewed as the generalised least-squares (LS) estimate while the second component is treated as the realisation of a Gaussian process. The ZWD can be modelled at time (t) as (Sacks et al., 1989):

$$ZWD(t)=\sum_{j=1}^{p}\beta_j h_j(t)+Z(t) \tag{15}$$

where h_j's are the pre-determined functions of time; p is the number of unknown parameter; β_j's are unknown coefficients to be estimated. The Gaussian process, $Z(t)$, is assumed to have zero mean and a covariance that can be estimated as:

$$V_t=\mathrm{Cov}(t_{i1},t_{i2})=\sigma^2R(t_{i1},t_{i2}) \tag{16}$$

between times t_{i1} and t_{i2}; σ^2 is the a-priori variance of the model in Eq. (16), and $R(t_{i1},t_{i2})$ is the correlation, whose form can be given by:

$$R_t=R(t_{i1},t_{i2})=e^{\left(-\theta|t_{i1}-t_{i2}|^q\right)}\quad 0<q\le 2 \tag{17}$$

In this study, the variable q is selected to equal two to indicate Euclidian norm, whilst the unknown parameter θ is to be estimated. Additionally, the first component of Eq. (15) can be simplified as an unknown coefficient $\hat{\mu}$, and the ordinary Kriging model can be formulated as (Morris et al, 1995):

$$Z\hat{W}D(t)=\hat{\mu}+Z(t) \tag{18}$$

The use of $\hat{\mu}$, instead of $\sum_{j=1}^{p}\beta_j h_j(t)$, will result in less computational effort with no significant model degradation (Sacks et al., 1989).

Given a set of times $t = \{t_0, t_2, ..., t_n\}$ and the corresponding (n+1) vector of ZWD estimates, $ZWD(t) = \{ZWD(t_0), ZWD(t_2), ..., ZWD(t_n)\}^T$, the best linear unbiased predictor (BLUP) at time t_k can be written as (Sacks et al., 1989):

$$\hat{ZWD}(t_k) = \hat{\mu} + v_{t_k}^T V_t^{-1}(ZWD(t) - H\hat{\mu}) \tag{19}$$

where

$$(V_t)_{ij} = Cov[Z(t_i), Z(t_j)], \; v_{t_k}^T = \{Cov[Z(t_k), Z(t_1)] ...., Cov[Z(t_k), Z(t_n)]\}$$
$$\hat{\mu} = \left((H^T V H)^{-1} H^T V\right) ZWD(t) \tag{20}$$

and H being a (n+1) vector of ones. In general, σ^2 and θ in Eqs. (17) and (18) are unknowns. They can be estimated by a method equivalent to the empirical Bayes approach (Koehler and Owen, 1996), which finds the parameters that are most consistent with the observed data. Since $Z(t)$ is Gaussian, the maximum likelihood estimation (MLE) method can be used to estimate σ^2 and θ (Koehler and Owen, 1996). The MLE of σ^2 is given as:

$$\hat{\sigma}^2 = \frac{(ZWD(t) - \hat{\mu}H)^T R_t^{-1} (ZWD(t) - \hat{\mu}H)}{n+1} \tag{21}$$

The maximum likelihood estimation of θ is a one-dimensional optimisation problem of the form:

$$\max_{\theta \in R^1} (-1/2)[(n \ln \hat{\sigma}^2) + \ln(\det(R_t))],$$

subject to $0 \le \theta \le \infty$ (22)

A nonlinear optimisation subroutine can usually solve Eq. (22) with respect to the parameter θ (Koehler and Owen, 1996). Once the optimal value of θ is obtained, it can then be substituted back into Eq. (17), and be used to determine V_t and $\hat{\mu}$. The predictor $\hat{ZWD}(t_k)$ in Eq. (19) can then be completely determined.

4 TESTING AND ANALYSIS OF METHODS FOR ESTIMATING MISSING ZENITH WET DELAY OBSERVATIONS

4.1 Test Description

The purpose of this section is to identify the best method of interpolating ZWD data for missing periods or when processing data at a different interval from which ZWD are available. The performances of all the aforementioned interpolation methods given in Sections 3.1-3.6 are assessed and inter-comparisons between the models are made using the ONSA ZWD data for the period September 10-22, 2004. The ZWD data is determined from a solution of GNSS data of a baseline between the IGS stations Onsala- Wettzell (ONSA-WZTR). The baseline length between the two stations is approximately 920km, which allows the “absolute” tropospheric estimation to be determined. The two stations were constrained to within 0.0001m. The data were collected for a 3-hr window session with sampling interval of the data was 5 minutes. The data were processed with the Bernese GNSS software package (Hugentobler et al., 2001). Data included in the processing also comprises the IGS products concerning the monitoring stations, satellite ephemerides, Earth Orientation Parameters, coordinates and velocity of ground stations, antenna phase centre offsets and variations. During processing, satellite and receiver clock offsets and the tropospheric zenith delay were estimated. The processing parameters include a cut-off elevation angle of 15 degrees,

the use of Niell mapping functions (Niell, 1996) and the Saastamoinen tropospheric model (Saastamoinen, 1972), which was employed to provide a-priori ZTD estimates. The observations were weighted using the elevation-angle dependent model. The ionosphere-free linear combination was implemented to mitigate the ionospheric residual errors. The final GNSS solution produced ZWD with RMSE of 12 mm. Figure 4 shows the time sequence of the ZWD data used in this study.

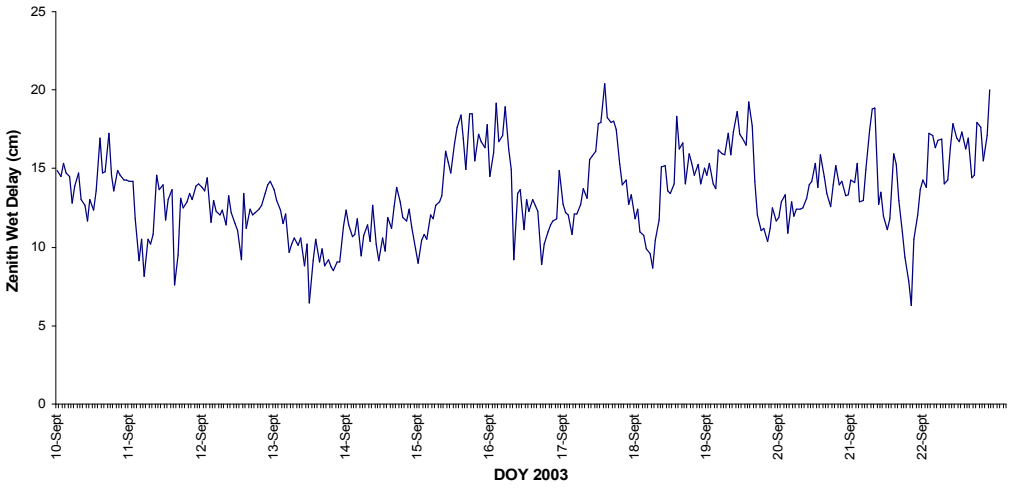

Figure 4: GNSS ZWD estimates at ONSA

The number of ZWD observations used to generate the interpolation models impacts the determination of the model coefficients, and consequently the accuracy of the interpolated ZWD observations. Thus, in this investigation, different sets of observations were used to construct the tested models. The number of pre-determined data points, m_{ZWD}, used to generate these models ranged from 4 to 48, i.e. $m_{ZWD} \in \{4, 6, 8, 12, 18, 24, 30, 36, 40, 44, 48\}$. Additionally, in each of these runs, the tested models were used to estimate one, two-consecutive, three-consecutive and four-consecutive missing observations, i.e. $1 \le k_{mis} \le 4$. The models were generated and analysed using the following procedure:

- Assuming a total of n observations in the data set, let k_{mis} be the pre-determined number of missing data points, where the interpolation is assumed performed to recover missing data, and m_{ZWD} the number of data points used to generate the model.
- Set $i = \frac{m_{ZWD}}{2}$.
- Let $ZWD_{mis}(t) = \{t_j, ZWD(t_j)\}_{j=i+1}^{i+k_{mis}}$ be the consecutively selected missed ZWD data set.
- Let $ZWD_{obs} = \{ZWD(t_{i-k_{mis}+1}), ZWD(t_i), ZWD(t_{i+k_{mis}+1}), ..., ZWD(t_{2i+k_{mis}})\}$ be the selected data set used to generate the models.
- Generate the IM or LS model based on the data set ZWD_{obs} and estimate the wet delay $\hat{ZWD}(t_j)$ for $\{t_j\}_{j=i+1}^{i+k_{mis}}$.
- To assess the model used at any epoch, the difference between the known ZWD at station ONSA, assumed as "truth", and the estimated ZWD, i.e. $\Delta ZWD_{diff}(t) = \hat{ZWD}(t) - ZWD_{mis}(t)$, is computed.
- Similarly, the next missing data points are estimated by shifting one position in time, i.e. $\{t_{j+1}, ZWD(t_{j+1})\}$ becomes $\{t_j, ZWD(t_{j+1})\}_{j=i+2}^{i+k_{mis}+1}$, until the last missing data point has been reached.

The above procedure places the set of missing ZWD observations, $ZWD_{mis}(t)$, in the centre of the modelling data set, $ZWD_{obs}(t)$. The first set of missing data begins at time $\{t_{i+1}, \ldots, t_{i+k_{mis}}\}$ and the last set finishes at time $\{t_{n-i-k_{mis}+1}, \cdots, t_{n-i}\}$. In all, a total of $(n - m_{ZWD} - k_{mis})$ missing data sets are considered. Given that there are k_{mis} missing observations in each of these sets, the total number of comparisons is therefore, $k_{mis}(n - m_{ZWD} - k_{mis})$. When all cases of missing data sets for a given model have been considered, the RMSE of the $k_{mis}(n - m_{ZWD} - k_{mis})$ ZWD differences are then calculated by:

$$RMSE_l = \sqrt{\frac{\sum_{j=1}^{k_{mis}(n-m_{ZWD}-k_{mis})} \left[\Delta ZWD_{diff}(t_j)\right]^2}{k_{mis}(n - m_{ZWD} - k_{mis})}} \tag{23}$$

Models with low RMSEs were considered as the most ideal interpolation models. For these models, a repeated-measures ANOVA (e.g. Walpole et al., 2007) was implemented as a follow-up test to determine whether there is a significant difference among them. For the repeated-measures ANOVA test, a p-value of less than 0.05 indicates a significant difference among the models.

4.2 Comparisons Between the Interpolation Models

In an effort to determine a suitable model for the purpose of estimating missing ZWDs, the interpolation models outlined in Section 3, were tested. The RMSEs, calculated via Eq. (23), of these models for $m_{ZWD} \in \{4, 6, 8, 12, 18, 24, 30, 36, 40, 44, 48\}$ are summarised in Tables 3-6. The results show that the Lagrange polynomials (LP) method is the poorest performer. As the number of data points increases, the LP exhibits what is known as Runge's phenomenon (Runge, 1901; Fornberg and Zuev, 2007), and thus produces poor outcomes. Runge's phenomenon is an error problem for a high-order polynomial interpolant on equidistant intervals, whereby the polynomial oscillates towards the end of the interval, as shown in Figure 5, resulting in poor ZWD estimation between the intervals. This effect was more prominent when estimating two, three and four missing ZWD observations.

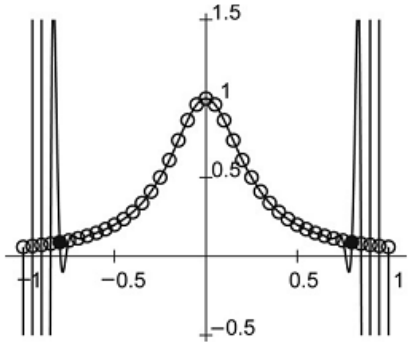

Figure 5 Runge's phenomenon (Fornberg and Zuev, 2007)

Table 3 RMSEs (cm) of the interpolated ZWDs for the case of a single missing observation

Num of Data Pts	Linear	Spline	CHP	FFT	Lagrange	Kriging
4	1.27	1.39	1.30	1.35	1.39	1.27
6	1.27	1.45	1.30	1.36	1.49	1.35
8	1.27	1.47	1.30	1.36	1.56	1.40
12	1.27	1.47	1.30	1.35	1.65	1.37
18	1.27	1.47	1.30	1.33	1.72	1.40
24	1.27	1.47	1.30	1.32	1.76	1.41
30	1.27	1.47	1.30	1.32	1.78	1.41
36	1.27	1.47	1.30	1.32	1.81	1.43
40	1.27	1.47	1.30	1.32	1.82	1.43
44	1.27	1.47	1.30	1.32	1.84	1.42
48	1.27	1.47	1.30	1.32	1.85	1.42

Table 4 RMSEs (cm) of the interpolated ZWDs for the case of two-successive missing observations

Num of Data Pts	Linear	Spline	CHP	FFT	Lagrange	Kriging
4	1.41	1.66	1.46	1.48	1.66	1.41
6	1.41	1.79	1.46	1.51	1.96	1.58
8	1.41	1.87	1.46	1.52	2.28	1.54
12	1.41	1.89	1.46	1.54	2.88	1.58
18	1.41	1.89	1.46	1.54	3.65	1.59
24	1.41	1.89	1.46	1.54	4.26	1.65
30	1.41	1.89	1.46	1.54	4.78	1.68
36	1.41	1.89	1.46	1.54	5.22	1.71
40	1.41	1.89	1.46	1.54	5.48	1.73
44	1.41	1.89	1.46	1.54	5.73	1.75
48	1.41	1.89	1.46	1.53	5.97	1.75

Table 5 RMSEs (cm) of the interpolated ZWDs for the case of three-successive missing observations

Num of Data Pts	Linear	Spline	CHP	FFT	Lagrange	Kriging
4	1.50	1.76	1.53	1.55	1.76	1.54
6	1.50	1.88	1.53	1.55	2.12	1.53
8	1.50	1.94	1.53	1.55	2.54	1.55
12	1.50	1.96	1.53	1.55	3.59	1.66
18	1.50	1.96	1.53	1.54	5.57	1.72
24	1.50	1.96	1.53	1.54	7.76	1.82
30	1.50	1.96	1.53	1.54	10.01	1.88
36	1.50	1.96	1.53	1.54	12.29	1.93
40	1.50	1.96	1.53	1.54	13.81	1.95
44	1.50	1.96	1.53	1.54	15.31	1.98
48	1.50	1.96	1.53	1.54	16.81	1.99

Table 6 RMSEs (cm) of the interpolated ZWDs for the case of four-successive missing observations

Num of Data Pts	Linear	Spline	CHP	FFT	Lagrange	Kriging
4	1.62	2.12	1.68	1.68	2.12	1.65
6	1.62	2.35	1.68	1.70	2.99	1.71
8	1.62	2.48	1.68	1.71	4.02	1.73
12	1.62	2.51	1.68	1.71	6.45	1.81
18	1.62	2.51	1.68	1.71	11.03	1.87
24	1.62	2.51	1.68	1.70	16.62	1.98
30	1.62	2.51	1.68	1.70	23.04	2.06
36	1.62	2.51	1.68	1.71	30.20	2.10
40	1.62	2.51	1.68	1.71	35.42	2.13
44	1.62	2.51	1.68	1.70	41.04	2.16
48	1.62	2.51	1.68	1.70	47.04	2.17

Tables 3-6 also indicate that the linear interpolation (LI), the cubic Hermite polynomial (CHP) and fast Fourier transform (FFT) models (interpolants that are dependent only on the most recent pair of data points) produce better estimates than splines and ordinary Kriging, which estimate the missing data points by giving greater weights to more recent data points, and lesser weights to those that are further away. Kriging did, however, produce comparable results to these models when the number of modelling data is low. The LI model, which was the simplest of all to use, produced the best results across all scenarios. The LI provided, on average, ZWD estimates to within 1.3 cm to 1.6 cm from the actual ZWD data, which corresponds to a PWV error of about 2 mm to 2.5 mm. This level of discrepancy is comparable to many GNSS PWV studies (e.g., Basili et al., 2002; Snajdrova et al., 2006; Wang et al., 2007). Note that both LI and CHP are methods that utilise the two most recent observations, with one on either side of the missing data set.

The favourable results for the LI, CHP and FFT models can be explained by the autocorrelation study in Section 2, whereby significant correlations occur among the estimates within a 1h to 2-h period. Successive 1-h ZWD estimates have an autocorrelation value as high as 0.8 h. Inclusion of several data points that are, time-wise, distant from the estimation time may have introduced noise into the splines and ordinary Kriging models.

Although the LI models appears to be best interpolation method based on its RMSE value, a repeated-measures ANOVA test was necessary for investigating whether it is statistical superior to the CHP and FFT methods. The results of the ANOVA test are given in Table 7. The table shows that the p-values for all the cases considered here were significantly greater than 0.05, which strongly suggest that there is no statistical difference in the performances among the LI, CHP and FFT interpolation models. Hence, the overall RMSE and the ANOVA results summarise that the LI is marginally, but not statistically, better than the CHP and FFT models.

Table 7 P-values of repeated-measure ANOVA test for LI, CHP and FFT interpolation methods

Number of data points used	Number of Missing Observations			
	One	Two	Three	Four
4	0.772	0.893	0.869	0.973
6	0.752	0.832	0.896	0.999
8	0.806	0.866	0.913	0.999
12	0.806	0.863	0.922	0.998
18	0.824	0.866	0.925	0.997
24	0.823	0.87	0.925	0.997
30	0.824	0.87	0.926	0.997
36	0.824	0.873	0.927	0.996
40	0.824	0.873	0.927	0.996
44	0.825	0.874	0.927	0.996
48	0.825	0.875	0.927	0.996

5 CONCLUSIONS

In the efforts to determine the most appropriate models for the interpolation and prediction of ZWD estimates, an autocorrelation analysis of the tropospheric estimates time series was initially carried out on the WVR ZWD estimates at ONSA. The autocorrelation study was restricted to a 12-h time period to ensure a degree of stationarity in the time series. It was found that the time lag for significant autocorrelation was observed within 2 hours. If a Gauss Markov model is assumed, this value can be of significant help in dynamic modelling of ZWD in recursive techniques such as Kalman Filtering.

An investigation into the performance of several modelling techniques was carried out to determine the best approach for estimating missing data points for a set of ZWD observations. Such interpolation processes are needed for post processing applications. For the investigated data set, the RMSE results indicate that the LI model generated the best interpolation results and thus no complex models are needed for the interpolation of ZWD. The favourable results for the LI model, which only depends on the two most recent data points, were reflected in the autocorrelation plot of the ZWD estimates, whereby significant autocorrelation values were observed for up to 2-h only. Although a follow-up ANOVA test indicate that there is no statistical difference in the performances of the LI model in comparison to the CHP and FFT models, the ease-of-use of the LI model ensures that it is still the recommended interpolation method.

REFERENCES

Basili, P., Bonafoni, S., Mattioli, V., Ciotti, P. and Fionda, E. (2002). A ground-based microwave radiometer and a GPS network for the remote sensing of atmospheric water vapour content: a year of experimental results. 1st COST720 Workshop: Integrated ground based remote sensing stations for atmospheric profiling. l'Aquila, Italy, 18-21 June 2002.

Benesty, J., Chen, J. and Huang, Y. (2004). Time-delay estimation via linear interpolation and cross correlation. IEEE Transactions on Speech and Audio Processing, 12 (5), 509-519.

Borre, K. and Tiberius, C. (2000). Time series analysis of GPS observables. Proceedings of the 11th International Technical Meeting of the Satellite Division of The Institute of Navigation, Salt Lake City, Utah, 19-22 September 2000.

Burden, R. L. and Faires, J.D. (2004). Numerical Analysis. 8th ed. Pacific Grove: Brooks/Cole Publishing Company.

Fornberg, B. and Zuev, J. (2007). The Runge phenomenon and spatially variable shape parameters in RBF interpolation. Computers & Mathematics with Applications, 54 (3), 379-398.

Frigo, M., and Johnson, S.G. (1998). FFTW: An adaptive software architecture for the FFT. Proceedings of the International Conference on Acoustics, Speech, and Signal Processing 3, Seattle, USA, 12-15 May 1998, 1381-1384.

Gutman, S. I., and Benjamin, S.G. (2001). The Role of Ground-Based GPS Meteorological Observations in Numerical Weather Prediction. GPS Solutions, 4 (4), 16-24.

Gutman, S. I., Sahm, S.R., Benjamin, S.G., Schwartz, B.E., Holub, K.L., Stewart, J.Q. and Smith, T.L. (2004). Rapid retrieval and assimilation of ground based GPS precipitable water observations at the NOAA forecast systems laboratory: Impact on weather forecasts. Journal of the Meteorological Society of Japan, 82 (1B), 351-360.

Haefele, P., L. Martin, M. Becker, E. Brockmann, J. Morland, S. Nyeki, C. Matzler, and M. Kirchner. (2004). Impact of radiometric water vapor measurements on troposphere and height estimates by GPS. ION GNSS-04 Proceedings, Long Beach, California, 21-24 September 2004.

Hugentobler, U., S. Schaer, and P. Fridez, eds. (2001). Bernese GPS software version 4.2: Astronomical Institute University of Berne.

Liu, J., Sun, Z., Liang, H., Xu, X. and Wu, P. (2005). Precipitable water vapor on the Tibetan plateau estimated by GPS, water vapor radiometer, radiosonde, and numerical weather prediction analysis and its impact on the radiation budget. Journal of Geophysical Research, 110, D17106.

Macpherson, S. R., Deblonde, G., Aparicio, J.M. and Casati, B. (2007). Impact of NOAA ground-based GPS observations on the Canadian regional analysis and forecast system. Monthly Weather Review, 136 (7), 2727-2745.

Mattioli, V., Westwater, E.R. Gutman, S.I. and Morris, V.R. (2005). Forward model studies of water vapor using scanning microwave radiometers, global positioning system, and radiosondes during the cloudiness intercomparison experiment. IEEE Transactions on Geoscience and Remote Sensing, 43 (5), 1012-1021.

Niell, A. E. (1996). Global mapping functions for the atmosphere delay at radio wavelenghts. Journal of Geophysical Research, 101 (B2): 3227-3246.

Koehler, J. R. and Owen, A.B. (1996). Computer experiments. In Handbook of Statistics, ed. S. Ghosh and C. R. Rao, 261-305. New York: Elsevier Science.

Kuo, Y. H., Zou, X. and Guo, Y. R. (1996). Variational assimilation of precipitable water using a nonhydrostatic mesoscale adjoint model. Monthly Weather Review 124 (1): 122-147.

Runge, C. (1901). Über empirische Funktionen und die Interpolation zwischen äquidistanten Ordinaten. Zeitschrift für Mathematik und Physik, 46, 224-243.

Saastamoinen, J. (1973). Contributions to the theory of atmospheric refraction. Bullétin Géodésique 105, 106, 107: 279-298, 383-397, 13-34.

Sacks, J., Welsh,W.J., Mitchell, T. J. and Wynn, H. P. (1989). Design and analysis of computer experiments. Statistical Science, 4 (4), 409-423.

Smith, T. L., Benjamin, S. G., Gutman, S. I. and Sahm, S. (2006). Short-range forecast impact from assimilation of GPS-IPW observations into the Rapid Update Cycle. Monthly Weather Review, 135 (8), 2914–2930.

Snajdrova, K., Boehm, J., Willis, P., Haas, R. and Schuh, H. (2006). Multi-technique comparison of tropospheric zenith delays derived during the CONT02 campaign. Journal of Geodesy, 79 (10-11), 613–623.

Stoew, B., Nilsson, T., Elgered, G. and Jarlemark. (2007) P. O. J. Temporal correlations of atmospheric mapping function errors in GPS estimation. Journal of Geodesy, 81 (5), 311-323.

Vedel, H. and Huang X. Y. (2003). A NWP impact study with ground based GPS data. The International Workshop on GPS Meteorology. Tsubaka, Japan, 14-17 January 2003.

Vedel, H. and Huang, X.Y. (2004). Impact of ground-based GPS data on numerical weather prediction. Journal of Meteorological Society of Japan 82 (1B), 459-472.

Walpole, R. E., R. Myers, and S. L. Myers (2007). Probability and Statistics for Engineers and Scientists. 8th ed. London, Prentice-Hall.

Wang, J., Zhang, L., Dai, A., van Hove, T. and van Baelen, J. (2007). A near-global, 2-hourly data set of atmospheric precipitable water from ground-based GPS measurements. Journal of Geophysical Research, 112, D11107.

Wei, W. (2006). Time series analysis - Univariate and multivariate methods. 2nd ed. USA, Pearson Education, Inc.